LETTERS

A single sub-kilometre Kuiper belt object from a stellar occultation in archival data

H. E. Schlichting[1,2], E. O. Ofek[1], M. Wenz[3], R. Sari[1,4], A. Gal-Yam[5], M. Livio[6], E. Nelan[6] & S. Zucker[7]

The Kuiper belt is a remnant of the primordial Solar System. Measurements of its size distribution constrain its accretion and collisional history, and the importance of material strength of Kuiper belt objects[1–4]. Small, sub-kilometre-sized, Kuiper belt objects elude direct detection, but the signature of their occultations of background stars should be detectable[5–9]. Observations at both optical[10] and X-ray[11] wavelengths claim to have detected such occultations, but their implied abundances are inconsistent with each other and far exceed theoretical expectations. Here we report an analysis of archival data that reveals an occultation by a body with an approximately 500-metre radius at a distance of 45 astronomical units. The probability of this event arising from random statistical fluctuations within our data set is about two per cent. Our survey yields a surface density of Kuiper belt objects with radii exceeding 250 metres of $2.1^{+4.8}_{-1.7} \times 10^7$ deg^{-2}, ruling out inferred surface densities from previous claimed detections by more than 5σ. The detection of only one event reveals a deficit of sub-kilometre-sized Kuiper belt objects compared to a population extrapolated from objects with radii exceeding 50 kilometres. This implies that sub-kilometre-sized objects are undergoing collisional erosion, just like debris disks observed around other stars.

A small Kuiper belt object (KBO) crossing the line of sight to a star will partially obscure the stellar light, an event which can be detected in the star's light curve. For visible light, the characteristic scale of diffraction effects, known as the Fresnel scale, is given by $(\lambda a/2)^{1/2} \approx 1.3$ km, where $a \approx 40$ astronomical units (AU) is the distance to the Kuiper belt and $\lambda \approx 600$ nm is the wavelength of our observations.

Diffraction effects will be apparent in the star's light curve as a result of occulting KBOs provided that both the star and the occulting object are smaller than the Fresnel scale[12,13]. Occultations by objects smaller than the Fresnel scale are in the Fraunhofer regime. In this regime the diffraction pattern is determined by the size of the KBO and its distance to the observer, the angular size of the star, the wavelength range of the observations and the impact parameter between the star and the KBO (see Supplementary Information for details). The duration of the occultation is approximately given by the ratio of the Fresnel scale to the relative velocity perpendicular to the line of sight between the observer and the KBO. Because the relative velocity is usually dominated by the Earth's velocity around the Sun, which is 30 km s^{-1}, typical occultations only last a short time of the order of a tenth of a second.

Extensive ground-based efforts have been conducted to look for optical occultations[9,10,14,15]. So far, these visible searches have announced no detections in the region of the Kuiper belt (30–60 AU), but one of these quests claims to have detected some events beyond 100 AU and at about 15 AU (ref. 10). Unfortunately, ground-based surveys may suffer from a high rate of false-positives owing to atmospheric scintillation, and lack the stability of space-based platforms. The ground-breaking idea to search for occultations in archival RXTE X-ray data resulted in several claimed occultation events[11]. Later, revised analysis of the X-ray data[16–19] concluded that the majority of the originally reported events are most probably due to instrumental dead-time effects. Thus, previous reports of optical and X-ray events remain dubious[14] and their inferred KBO abundance is inconsistent with the observed break in the KBO size distribution, which was obtained from direct detections of large KBOs[20–22]. Furthermore, they are also difficult to reconcile with theoretical expectations, which predict collisional evolution for KBOs smaller than a few kilometres in size[4,23] and hence a lower KBO abundance than inferred from extrapolation from KBOs with radii $r > 50$ km.

For the past 14 years, the Fine Guidance Sensors (FGS) on board the Hubble Space Telescope (HST) have been collecting photometric measurements of stars with 40-Hz time resolution, allowing for the detection of the occultation diffraction pattern rather than a simple decrease in the photon count. We examined four and a half years of archival FGS data, which contain about 12, 000 star hours of low ecliptic latitude ($|b| < 20^\circ$) observations.

Our survey is most likely to detect occultations by KBOs that are 200–500 m in radius given the signal-to-noise of our data (Supplementary Fig. 1) and a power-law size distribution with power-law index between 3 and 4.5. Occultation events in this size range are in the Fraunhofer regime, where the diffraction pattern is independent of the occulting object's shape and the depth of the diffraction pattern varies linearly with the area of the object. The theoretical light curves for our search algorithm were therefore calculated in this regime. We fitted these theoretical occultation templates to the FGS data and performed χ^2 analysis to identify occultation candidates (see Supplementary Information). We detected one occultation candidate, at ecliptic latitude 14°, that significantly exceeds our detection criterion (Fig. 1). The best-fit parameters yield a KBO size of $r = 520 \pm 60$ m and a distance of 45^{+5}_{-4} AU where we assumed a circular KBO orbit and an inclination of 14°. Using bootstrap simulations, we estimate a probability of ~2% that such an event is caused by statistical fluctuations over the whole analysed FGS data set (Supplementary Fig. 5). We note that for objects on circular orbits around the Sun two solutions can fit the duration of the event. However, the other solution is at a distance of 0.07 AU from the Earth, and is therefore unlikely. It is also unlikely that the occulting object was located in the asteroid belt, because the expected occultation rate from asteroids is about two orders of magnitude less than our implied rate. Furthermore, an asteroid would have to have an eccentricity of order unity to be able to explain the duration of the observed occultation event.

Using the KBO ecliptic latitude distribution from ref. 24, our detection efficiency, and our single detection, we constrain the surface

[1]Department of Astronomy, 249-17, California Institute of Technology, Pasadena, California 91125, USA. [2]CITA, University of Toronto, 60 St George Street, Ontario, M5S 3H8, Canada. [3]Goddard Space Flight Center, 8800 Greenbelt Road, Greenbelt, Maryland 20771, USA. [4]Racah Institute of Physics, Hebrew University, Jerusalem 91904, Israel. [5]Faculty of Physics, Weizmann Institute of Science, POB 26, Rehovot 76100, Israel. [6]Space Telescope Science Institute, 3700 San Martin Drive, Baltimore, Maryland 21218, USA. [7]Department of Geophysics and Planetary Sciences, Tel Aviv University, Tel Aviv 69978, Israel.

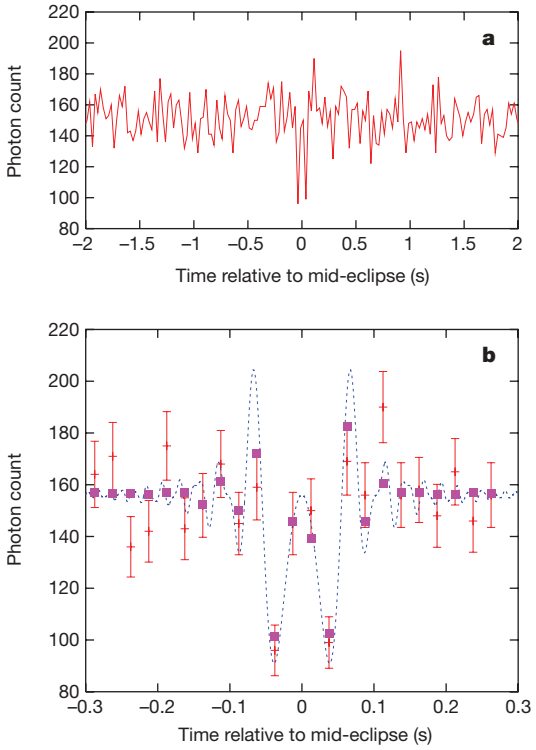

Figure 1 | Photon counts as a function of time of the candidate occultation event observed by FGS2. **a**, The photon count spanning ±2 s around the occultation event. **b**, The event in detail. The red crosses are the FGS data points with Poisson error bars, the dashed blue line is the theoretical diffraction pattern (calculated for the 400–700 nm wavelength range of the FGS observations), and the pink squares correspond to the theoretical light curve integrated over 40-Hz intervals. We note that the actual noise for this observation is about 4% larger than Poisson noise owing to additional noise sources such as dark counts (about 3–6 counts in a 40-Hz interval), and jitter caused by the displacement of the guide star (by up to 10 mas) from its null position. The mean signal-to-noise ratio in a 40-Hz interval for the roughly half an hour of observations is ~12. The event occurred at Coordinated Universal Time UTC 05:17:49 on 24 March 2007. The best-fit χ^2 is 20.1 with 21 degrees of freedom. The star has an ecliptic latitude of +14. Its angular radius and effective temperature are about 0.3 of the Fresnel scale and about 4,460 K, respectively. These values were derived by fitting the 2MASS[26] JHK and USNO-B1 BR[27] photometry with a black-body spectrum. The position of the star is RA = 186.87872°, dec. = 12.72469° (J2000) and its estimated V-magnitude is 13.4. The auto-correlation function (excluding lag zero) of the photometric time series of this event is consistent with zero within the statistical uncertainty. Each FGS provides two independent photomultiplier (PMT) readings and we confirmed that the occultation signature is present in both of these independent photon counts. We examined the photon counts of the other guide star that was observed by FGS1 at the time of the occultation and confirmed that the occultation signal is only present in the observations recorded by FGS2. We examined the engineering telemetry for HST around the time of the event and verified that the guiding performance of HST was normal. We therefore conclude that the above occultation pattern is not caused by any known instrumental artefacts.

density around the ecliptic (averaged over $-5^\circ < b < 5^\circ$) of KBOs with radii larger than 250 m to $2.1^{+4.8}_{-1.7} \times 10^7$ deg^{-2} (see Supplementary Information Sections 5 and 6). This surface density is about three times the implied surface density at 5.5° ecliptic latitude and about five times the surface density at 8–20° ecliptic latitude. This is the first measurement of the surface density of hectometre-sized KBOs and it improves previous upper limits by more than an order of magnitude[9,15].

Figure 2 displays our measurement for the sub-kilometre KBO surface density and summarizes published upper limits from various surveys. Our original data analysis focused on the detection of KBOs located at the distance of the Kuiper belt between 30 AU and 60 AU. To compare our results with previously reported ground-based detections

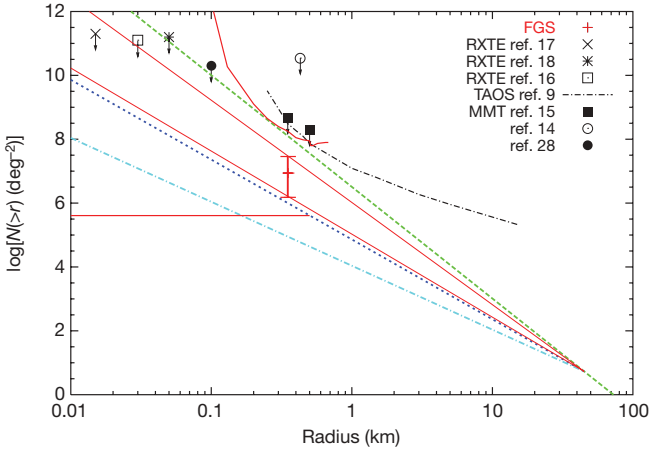

Figure 2 | Cumulative KBO size distribution as a function of KBO radius for objects located between 30 and 60 AU. The results from our FGS survey are shown in red and are presented in three different ways. (1) The red cross is derived from our detection and represents the KBO surface density around the ecliptic (averaged over $-5^\circ < b < 5^\circ$) and is shown with 1σ error bars. The cross is plotted at $r = 250$ m, which is roughly the peak of our detection probability (see Supplementary Information Section 6 for details). (2) The upper and lower red curves correspond to our upper and lower 95% confidence levels which were derived without assuming any size distribution. (3) The region bounded by the two straight red lines falls within 1σ of our best estimate for the power-law size distribution index, that is, $q = 3.9 \pm 0.3$, which was calculated for low ecliptic latitudes ($|b| < 5^\circ$). These lines are anchored to the observed surface density at $r = 45$ km. For comparison, we also show three other lines (green, blue, turquoise). The green (long-dashed) line is the observed size distribution of large KBOs (that is, $r > 45$ km), which has $q = 4.5$, extrapolated as a single power-law to small sizes. The blue (short-dashed) line is a double power-law with $q = 3.5$ (collisional cascade of strength-dominated bodies) for KBOs with radii less than 45 km and $q = 4.5$ above. The turquoise (dot-dashed) line corresponds to $q = 3.0$ (collisional cascade of strengthless rubble piles) for KBOs below 45 km in size. All distributions are normalized to $N(>r) = 5.4$ deg^{-2} at a radius of 45 km (ref. 25). In addition, 95% upper limits from various surveys are shown in black (refs 17, 18, 16, 9, 15, 14 and 28). We note that a power-law index of 3.9 was used for calculating the cumulative KBO number density from the RXTE observations.

beyond 100 AU (ref. 10), we performed a second search of the FGS data that was sensitive to objects located beyond the classical Kuiper belt. Our results challenge the reported ground-based detections of two 300 m-sized objects beyond 100 AU (ref. 10). Given our total number of star hours and a detection efficency of 3% for 300-m-sized objects at ~100 AU we should have detected more than twenty occultations. We therefore rule out the previously claimed optical detections[10] by more than 5σ. This result accounts for the broad latitude distribution of our observations (that is, $|b| < 20^\circ$) and the quoted detection efficiency of our survey includes the effect of the finite angular radii of the guide stars at 100 AU.

The KBO cumulative size distribution is parameterized by $N(>r) \propto r^{1-q}$, where $N(>r)$ is the number of objects with radii greater than r, and q is the power-law index. The power-law index for KBOs with radii above ~45 km is ~4.5 (refs 21, 22) and there is evidence for a break in the size distribution at about $r_{\rm break} \approx 45$ km (refs 20–22). Hence we use this break radius and assume a surface density for KBOs larger than $r_{\rm break}$ (ref. 25) of 5.4 deg^{-2} around the ecliptic. Accounting for our detection efficiency, the velocity distribution of the HST observations, and assuming a single power-law for objects with radii less than 45 km in size, we find $q = 3.9^{+0.3,+0.4}_{-0.3,-0.7}$ (1σ and 2σ errors) below the break. Our results firmly show a deficit of sub-kilometre-sized KBOs compared to large objects. This confirms the existence of the previously reported break and establishes a shallower size distribution extending two orders of magnitude in size down to sub-kilometre-sized objects. This suggests that sub-kilometre-sized KBOs underwent collisional evolution, eroding the smaller KBOs.

This collisional grinding in the Kuiper belt provides the missing link between large KBOs and dust, producing debris disks around other stars. Currently, our results are consistent with a power-law index of strength-dominated collisional cascade[23], $q = 3.5$, within 1.3σ and with predictions for strengthless rubble piles[4], $q = 3.0$, within 2.4σ. An intermediate value of $3 < q < 3.5$ implies that KBOs are strengthless rubble piles above some critical size, $r_c < r < 45$ km, and strength-dominated below it, $r < r_c$. Our observations constrain r_c for the first time to our knowledge. At the 2σ level we find $r_c > 3$ km.

Using our estimate for the size distribution power-law index ($q = 3.9$) and our KBO surface density for 250-m-sized KBOs at an ecliptic latitude of $b = 5.5^\circ$, which is the ecliptic latitude of the RXTE observations of Scorpius X-1, we predict that there should be about 3.6×10^9 objects of radius 30 m per square degree. This is about 150 times less than the original estimate from X-ray observations of Scorpius X-1 that reported 58 events[11], and it is about 30 times less than the revised estimate from the same X-ray observations, which concludes that up to 12 events might be actual KBO occultations[16]. Our results rule out the implied surface density from these 12 events at 7σ confidence level. One can reconcile our results and the claimed X-ray detections only by invoking a power-law index of $q \approx 5.5$ between 250 m and 30 m. More recent X-ray work reports no new detections in the region of the Kuiper belt but places an upper limit of 1.7×10^{11} deg^{-2} for objects of 50 m in radius and larger[18]. This is consistent with the KBO surface density of $N(>50\,\mathrm{m}) = 8.2 \times 10^8$ deg^{-2} that we derive by extrapolating from our detection in the hectometre size range.

The statistical confidence level on our detection is 98%. However, our conclusions that there is a significant break in the size distribution and that collisional erosion is taking place and the significant discrepancy with previously claimed occultation detections rely on the low number of events we discovered. These conclusions would only be strengthened if this event was caused by an unlikely statistical fluctuation or an as-yet-unknown instrumental artefact.

Ongoing analysis of the remaining FGS data, which will triple the number of star hours, together with further development of our detection algorithm (that is, including a larger number of light-curve templates) holds the promise of additional detections of occultation events and will allow us to constrain the power-law index of the size distribution further.

Received 12 August; accepted 21 October 2009.

1. Davis, D. R. & Farinella, P. Collisional evolution of Edgeworth-Kuiper belt objects. *Icarus* **125,** 50–60 (1997).
2. Stern, S. A. & Colwell, J. E. Collisional erosion in the primordial Edgeworth-Kuiper belt and the generation of the 30–50 AU Kuiper gap. *Astrophys. J.* **490,** 879–882 (1997).
3. Kenyon, S. J. & Luu, J. X. Accretion in the early Kuiper belt. II. Fragmentation. *Astron. J.* **118,** 1101–1119 (1999).
4. Pan, M. & Sari, R. Shaping the Kuiper belt size distribution by shattering large but strengthless bodies. *Icarus* **173,** 342–348 (2005).
5. Bailey, M. E. Can 'invisible' bodies be observed in the Solar System? *Nature* **259,** 290–291 (1976).
6. Dyson, F. J. Hunting for comets and planets. *Q. J. R. Astron. Soc.* **33,** 45–57 (1992).
7. Axelrod, T. S., Alcock, C., Cook, K. H. & Park, H.-S. in *Robotic Telescopes in the 1990s* (ed. Filippenko, A. V.) 171–181 (1992).
8. Roques, F., Moncuquet, M. & Sicardy, B. Stellar occultations by small bodies—diffraction effects. *Astron. J.* **93,** 1549–1558 (1987).
9. Zhang, Z.-W. *et al.* First results from the Taiwanese-American Occultation Survey (TAOS). *Astrophys. J.* **685,** L157–L160 (2008).
10. Roques, F. *et al.* Exploration of the Kuiper belt by high-precision photometric stellar occultations: first results. *Astron. J.* **132,** 819–822 (2006).
11. Chang, H.-K. *et al.* Occultation of X-rays from Scorpius X-1 by small trans-neptunian objects. *Nature* **442,** 660–663 (2006).
12. Roques, F. & Moncuquet, M. A detection method for small Kuiper belt objects: the search for stellar occultations. *Icarus* **147,** 530–544 (2000).
13. Nihei, T. C. *et al.* Detectability of occultations of stars by objects in the Kuiper belt and Oort cloud. *Astron. J.* **134,** 1596–1612 (2007).
14. Bickerton, S. J., Kavelaars, J. J. & Welch, D. L. A Search for sub-km Kuiper belt objects with the method of serendipitous stellar occultations. *Astron. J.* **135,** 1039–1049 (2008).
15. Bianco, F. B. *et al.* A Search for occultations of bright stars by small Kuiper belt objects using Megacam on the MMT. *Astron. J.* **138,** 568–578 (2009).
16. Chang, H.-K., Liang, J.-S., Liu, C.-Y. & King, S.-K. Millisecond dips in the RXTE/PCA light curve of Sco X-1 and trans-Neptunian object occultation. *Mon. Not. R. Astron. Soc.* **378,** 1287–1297 (2007).
17. Jones, T. A., Levine, A. M., Morgan, E. H. & Rappaport, S. Production of millisecond dips in Sco X-1 count rates by dead time effects. *Astrophys. J.* **677,** 1241–1247 (2008).
18. Liu, C.-Y., Chang, H.-K., Liang, J.-S. & King, S.-K. Millisecond dip events in the 2007 RXTE/PCA data of Sco X-1 and the trans-Neptunian object size distribution. *Mon. Not. R. Astron. Soc.* **388,** L44–L48 (2008).
19. Blocker, A. W., Protopapas, P. & Alcock, C. R. A Bayesian approach to the analysis of time symmetry in light curves: reconsidering Scorpius X-1 occultations. *Astrophys. J.* **701,** 1742–1752 (2009).
20. Bernstein, G. M. *et al.* The size distribution of trans-neptunian bodies. *Astron. J.* **128,** 1364–1390 (2004).
21. Fuentes, C. I. & Holman, M. J. A SUBARU archival search for faint trans-neptunian objects. *Astron. J.* **136,** 83–97 (2008).
22. Fraser, W. C. *et al.* The Kuiper belt luminosity function from m(R)=21 to 26. *Icarus* **195,** 827–843 (2008).
23. Dohnanyi, J. W. Collisional models of asteroids and their debris. *J. Geophys. Res.* **74,** 2531–2554 (1969).
24. Elliot, J. L. *et al.* The Deep Ecliptic Survey: a search for Kuiper belt objects and centaurs. II. Dynamical classification, the Kuiper belt plane, and the core population. *Astron. J.* **129,** 1117–1162 (2005).
25. Fuentes, C. I., George, M. R. & Holman, M. J. A Subaru pencil-beam search for m(R) ~ 27 trans-neptunian bodies. *Astrophys. J.* **696,** 91–95 (2009).
26. Skrutskie, M. F. *et al.* The Two Micron All Sky Survey (2MASS). *Astron. J.* **131,** 1163–1183 (2006).
27. Monet, D. G. *et al.* The USNO-B catalog. *Astron. J.* **125,** 984–993 (2003).
28. Roques, F., Georgevits, G. & Doressoundiram, A. *The Kuiper Belt Explored by Serendipitous Stellar Occultations* 545–556 (University of Arizona Press, 2008).

Supplementary Information is linked to the online version of the paper at www.nature.com/nature.

Acknowledgements We thank H. K. Chang for comments that helped to improve this manuscript. Some of the numerical calculations presented here were performed on Caltech's Division of Geological and Planetary Sciences Dell cluster. Partial support for this research was provided by NASA through a grant from the Space Telescope Science Institute. R.S. acknowledges support from the ERC and the Packard Foundation. A.G.-Y. is supported by the Israeli Science Foundation, an EU Seventh Framework Programme Marie Curie IRG fellowship and the Benoziyo Center for Astrophysics, a research grant from the Peter and Patricia Gruber Awards, and the William Z. and Eda Bess Novick New Scientists Fund at the Weizmann Institute. S.Z. acknowledges support from the Israel Science Foundation–Adler Foundation for Space Research. E.O.O. is an Einstein Fellow.

Author Contributions H.E.S. wrote the detection algorithm, analysed the FGS data for occultation events, calculated the detection efficiency of the survey, preformed the bootstrap analysis and wrote the paper. E.O.O. calculated the stellar angular radii, the velocity information of the observations, the correlated noise and other statistical properties of the data. R.S. guided this work and helped with the scientific interpretation of the results. A.G.-Y. proposed using HST FGS data for occultation studies and helped to make the data available for analysis. M.W. extracted the FGS photometry streams and provided coordinates and magnitudes of the guide stars. M.L. helped in gaining access to the FGS data and provided insights into the operation and noise properties of the FGS. E.N. provided expert interpretation of the FGS photometric characteristics in the HST operational environment. S.Z. took part in the statistical analysis of the data. All authors discussed the results and commented on the manuscript.

Author Information Reprints and permissions information is available at www.nature.com/reprints. Correspondence and requests for materials should be addressed to H.E.S. (hes@astro.caltech.edu) or E.O.O. (eran@astro.caltech.edu).